

This version of the Electronic Supplementary Information replaces the version published on the 5th December 2018, which contained errors in Fig. S4.

## Supporting Information

### Activity Enhancement of Pt/MnO<sub>x</sub> Catalyst by Novel $\beta$ -MnO<sub>2</sub> for Low-temperature CO Oxidation: Study of the CO–O<sub>2</sub> Competitive Adsorption and Active Oxygen Species

Ningqiang Zhang,<sup>1</sup> Lingcong Li,<sup>1\*</sup> Rui Wu,<sup>1</sup> Liyun Song,<sup>1</sup> Lirong Zheng,<sup>3</sup> Guizhen Zhang,<sup>1</sup> Hong He<sup>1,2\*</sup>

1. Key Laboratory of Beijing on Regional Air Pollution Control, and Beijing Key Laboratory for Green Catalysis and Separation, Beijing University of Technology, Beijing 100124, P. R. China.

2. Collaborative Innovation Center of Electric Vehicles in Beijing, Beijing100081, P. R. China.

3. Beijing Synchrotron Radiation Facility, Institute of High Energy Physics, Chinese Academy of Sciences, Beijing 100049, P. R. China.

#### 1. Experiments

##### 1.1 Characterization

The crystal structures of the materials were identified by means of X-ray powder diffraction (XRD) over a Bruker D8 Advance X-ray diffractometer with Cu K $\alpha$  (1.5406 Å) radiation. The data were collected with a scanning speed of 2°/min and a step size of 0.02° over the angular range 2 $\theta$  (10° < 2 $\theta$  < 80°) at 40 kV and 40 mA. The data of the samples were analysed using the Rietveld refinement technique using the HighScore Plus program. The details of the Rietveld refinement steps are as follows: First, the phase structure was determined as follows: “strip *k*-Alpha2, determine background, search peaks, search and match (execute search and match), and chose the pdf code”. Second, Rietveld refinement was carried out as follows: “convert pattern to phase, Rietveld refinement based on the structure”, (1) automatic mode. Is the GOF-index scale below 2.0? If yes, the Rietveld refinement process completed. If no, continue the second step in the Rietveld refinement. (2) Semi-automatic mode. The steps are as follows: “use available background, zero shift, preferred orientation, scale factor, unit cell, U, V, W, peak shape, B overall, Extinction.” Repeat these steps until the GOF-index scale is below 2.0. The quality and

reliability of the Rietveld analysis were quantified using the corresponding figures of merit,  $R_{wp}$ , the statistically expected least-squares fit,  $R_{exp}$ , the profile residual,  $R_p$ , and the goodness of fit, GoF-index. A GoF scale below 2.0 means a perfect fitting. For the Pt/MnO<sub>x</sub> and Pt/MnO<sub>x</sub>-COM reduction at 1300 °C: 100 mg sample was treated under a 10 vol% H<sub>2</sub>/N<sub>2</sub> atmosphere in a tube furnace for 30 min and then encapsulated in N<sub>2</sub> at r.t.

Temperature-programmed desorption (TPD) experiments were carried out with Ar atmosphere in a quartz micro-reactor. The samples (30 mg) were pre-treated in a flow of Ar (30 ml min<sup>-1</sup>) at 300 °C for 30 min, and then cooled to room temperature with Ar as the temperature decreased to room temperature. The CO (1% CO, 99 % Ar), and/or O<sub>2</sub> (1% O<sub>2</sub>, 99% Ar) gases was then introduced with a flow rate of 50 ml min<sup>-1</sup> after the pretreatment to enable the gas adsorption, respectively. Then the sample were purged with Ar until the baseline to stable. The sample was heated from 30 °C to 1100 °C at a heating rate of 5 °C min<sup>-1</sup>. The m/z signals of 32 (O<sub>2</sub>), 28 (CO), and 44 (CO<sub>2</sub>) were monitored over a mass spectrometer (Hiden Analytical QGA). Co-adsorption of CO/O<sub>2</sub> and desorption experiments were carried out in the same equipment and procedure used as in CO-TPD as CO and O<sub>2</sub> (1% CO, 1% O<sub>2</sub>, 98% Ar) was used as the adsorbate.

The hydrogen temperature programmed reduction (H<sub>2</sub>-TPR) measurement was performed on a chemisorption analyzer (Auto Chem 2920) with a gas of 10% H<sub>2</sub>/N<sub>2</sub>. Total gas flow rate with 30 ml min<sup>-1</sup>. The temperature was increased linearly from 70 to 900 °C at a heating rate of 5 °C min<sup>-1</sup>. The H<sub>2</sub> consumption was recorded by TCD after removal of the produced H<sub>2</sub>O.

For the thermogravimetric analysis (TGA and DTGA), the samples were exposed to in a flow of H<sub>2</sub> (1.54%)/N<sub>2</sub> (50 ml min<sup>-1</sup>), with a heating rate of 10 °C min<sup>-1</sup>, from room temperature to 1300 °C with a heating rate of 10 °C min<sup>-1</sup>.

The chemical valences of the surface elements were investigated by X-ray photoelectron spectroscopy (XPS, ESCALAB 250XI) using Al K $\alpha$  as an exciting X-ray source. The spectra were calibrated with respect to the C 1s peak of adventitious carbon at 284.6 eV.

The images of transmission electron microscopy (TEM) and high resolution TEM

(HR-TEM) were collected over a JEOL transmission electron microscope (JEM-2100) operated at 200 kV.

The DRIFT spectra of the samples were obtained with a Thermo Scientific spectrometer (Tensor 27) at ambient temperature in the range of 4000–600  $\text{cm}^{-1}$  and at a resolution of 4  $\text{cm}^{-1}$ . The diffuse reflectance Fourier transform (DRIFT) spectra of CO adsorption and CO+O<sub>2</sub> co-adsorption over the catalysts were also collected over a FTIR spectrometer equipped with a Harrick accessory and a vacuum system.

Extend X-ray absorption fine structure spectroscopy (EXAFS) at the Pt K-edge was performed at the beamline 1W1B of the Beijing Synchrotron Radiation Facility (BSRF), Institute of High Energy Physics (IHEP), Chinese Academy of Sciences (CAS). The typical energy of the storage ring was 2.5 GeV with a maximum current of 250 mA. The Si (111) double crystal mono-chromator was used. The powdered sample was first pressed into sheet and loaded into a reactor cell equipped with polyimide windows.

A Raman Spectrometer (JY T64000, American) with a 532 nm wavelength excitation laser was used to measure the micro-Raman spectra. Pure powder supported on a sheet glass was used without any pretreatment.

## **1.2 Catalysts preparation**

All the chemicals employed herein were of analytical grade and used as received without further purification, while deionized water was used throughout. The commercial  $\beta$ -MnO<sub>2</sub> material was purchased from Huitong Hunan science and technology Co., LTD.

In a typical  $\beta$ -MnO<sub>2</sub> synthesis process, an aqueous solution (75 mL) containing MnSO<sub>4</sub>·H<sub>2</sub>O (2.4840 g), KMnO<sub>4</sub> (1.6590 g) and Zn(acac)<sub>2</sub> (11.62 mg, with Zn(acac)<sub>2</sub> being weighed using a thermo-gravimetric microbalance with a precision of 0.0001 mg) was poured into a 100 mL Teflon-lined stainless steel autoclave, which was subsequently sealed and maintained at 160 °C for 24 h. The resulting black slurries were filtered, washed with deionized water for four times, and subsequently dried at 110 °C for 24 h. All the samples were calcined at 500 °C in air for 6 h before use. Not any S, K, but only 0.005% Zn elements were detected by ICP-AES.

In a second step, Pt was loaded on the surface of  $\beta$ -MnO<sub>2</sub> through a deposition–precipitation method. The precursor (NH<sub>3</sub>)<sub>4</sub>Pt(NO<sub>3</sub>)<sub>2</sub> was dissolved in an aqueous solution containing  $\beta$ -MnO<sub>2</sub>. The pH value of the solutions was adjusted and fixed to 10.0 by adding NH<sub>3</sub> H<sub>2</sub>O. The solution was continuously stirred overnight. A black slurry was obtained by centrifuging the solution. The precipitate was washed with D.I. water for several times, dried at 70 °C for 8 h at ambient–pressure, and then calcinated at 300 °C for 6 h, giving the final products. Afterwards, a further calcination step at 300 °C was performed for 6 h to obtain the final products. While no significant changes in size or surface morphology were observed for the  $\beta$ -MnO<sub>2</sub> nano–rods and the  $\beta$ -MnO<sub>2</sub>–COM material after Pt loading, but a new Mn<sub>2</sub>O<sub>3</sub> crystal phase was observed. The formation of this new phase may be due to the reduction of Mn(IV) into Mn(III) over the Pt/MnO<sub>x</sub> catalyst. The actual Pt loadings of Pt were 0.83 wt% and 0.87 wt% for the Pt/MnO<sub>x</sub> and Pt/MnO<sub>x</sub>–COM catalysts, respectively, which were determined by inductively coupled plasma atomic emission spectroscopy (ICP–AES) analysis. The 1 wt% Pt/Al<sub>2</sub>O<sub>3</sub> sample was also prepared with the same procedure.

SEM-EDX images were obtained on a Hitachi S4800 field-emission SEM instrument with Super energy-dispersive X-ray spectroscopy (super-EDX) detector featuring a large solid angle (~1 sr) that enables X-ray count rate in excess of 100 kcps.. The MnO<sub>2</sub> samples were immobilized onto silicon wafers and to be dried in a vacuum desiccator for several hours and then treated by gold sputtering.

### 1.3 Catalytic performance

The catalytic performance of samples for CO oxidation were evaluated reactor in a quartz micro-reactor (id = 8 mm) at atmospheric pressure. The 80 mg of the catalyst (40-60 mesh size) was loaded in the reactor and a thermocouple was located in the middle of the catalyst bed to monitor the reaction temperature. The reactant feed was 1 vol% CO (inlet pressure 0.1 MPa) and 1 vol% O<sub>2</sub> (inlet pressure 0.1 MPa) in 98% N<sub>2</sub> with a flow rate of 25 ml min<sup>-1</sup> and corresponding space velocity of 18750 ml h<sup>-1</sup> g<sub>cat</sub><sup>-1</sup>. The effluent gases were detected on-line by a gas chromatograph (Shimadzu GC-2014C) equipped with a thermal conductivity detector and a 5 Å molecular sieve packed column.

The turnover frequency (TOF) and reaction rates were measured with a feed stream of 1 vol% CO/1 vol %O<sub>2</sub>/He, and gas space velocity in the range of 1.88×10<sup>4</sup>-3.0×10<sup>5</sup> ml h<sup>-1</sup> g<sub>cat</sub><sup>-1</sup>. The conversion of CO was kept below 15% in order to calculate the reaction rates under differential reaction conditions.

Kinetic measurements were conducted with feed streams of 0.5-5 vol% CO and 0.5-5 vol% O<sub>2</sub> balanced with He, and the CO conversions were adjusted to below 15% by varying the gas space velocity to calculate the reaction rates under differential reactor conditions.

The CO conversions were calculated based on the difference between inlet and outlet concentrations.

$$\text{CO conversions} = (\text{CO}_{\text{inlet}} - \text{CO}_{\text{outlet}}) / \text{CO}_{\text{inlet}} \times 100\%$$

## 2. Figures

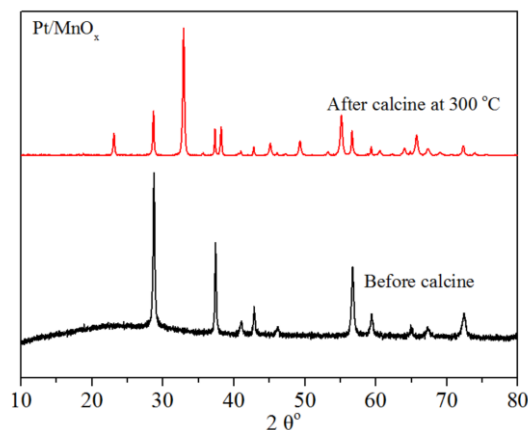


Figure S1. The XRD patterns of the Pt/MnO<sub>x</sub> sample. Before (black) after (red) calcine.<sup>1</sup>

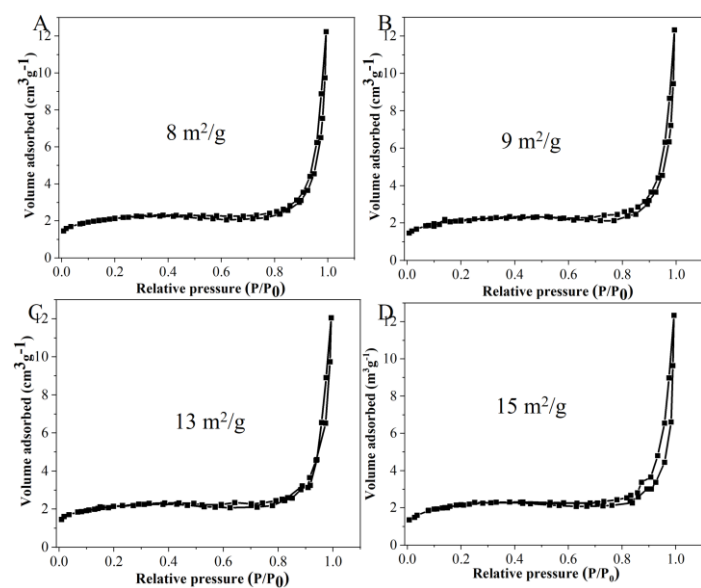


Figure S2. Nitrogen adsorption–desorption isotherms of  $\beta$ -MnO<sub>2</sub> (A), Pt/MnO<sub>x</sub> (B),  $\beta$ -MnO<sub>2</sub>-COM (C), and Pt/MnO<sub>x</sub>-COM (D) samples.

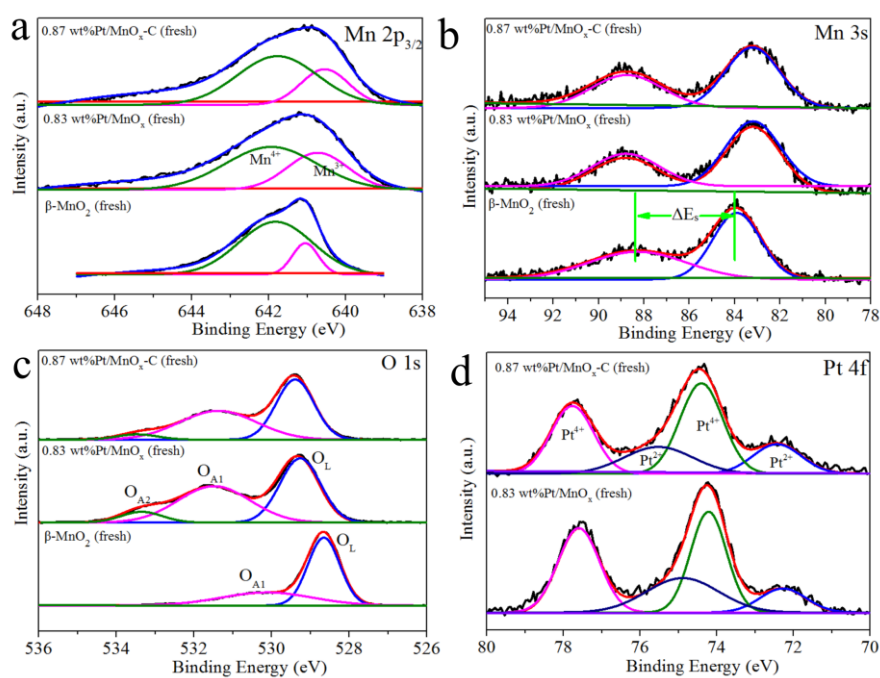


Figure S3. XPS spectra of Mn 2p<sub>3/2</sub> (a), Mn 3s (b), O 1s (c), and Pt 4f (d) over the fresh catalysts.<sup>1</sup>

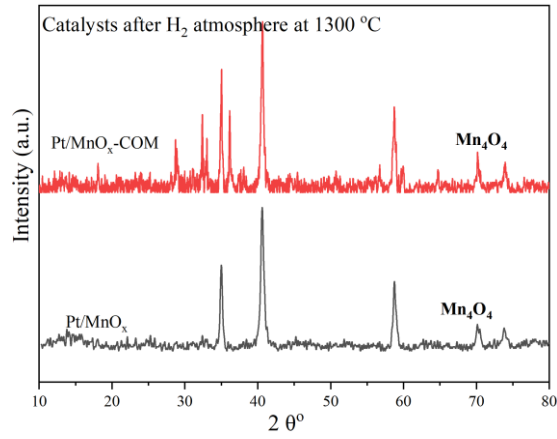


Figure S4. The XRD patterns of Pt/MnO<sub>x</sub> and Pt/MnO<sub>x</sub>-COM catalysts after H<sub>2</sub> atmosphere at 1300 °C.<sup>1</sup>

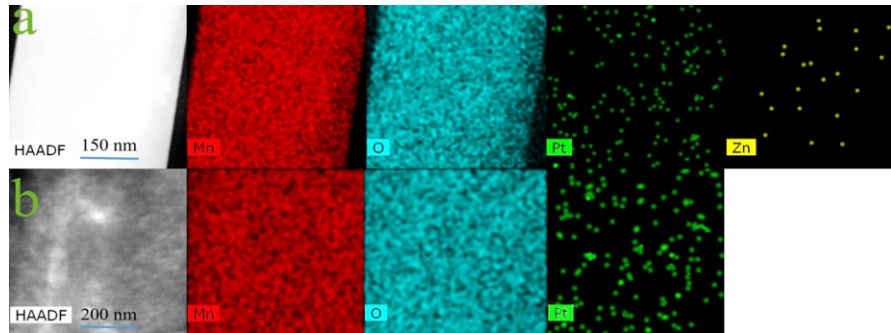


Figure S5. HAADF-STEM-EDX mapping images of the fresh Pt/MnO<sub>x</sub> (a, b) and Pt/MnO<sub>x</sub>-COM (c, d) catalysts.

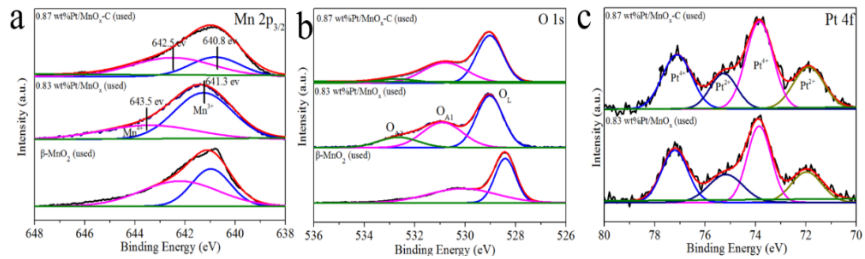


Figure S6. XPS spectra of Mn 2p<sub>3/2</sub> (a), O 1s (b), and Pt 4f over the spent catalysts<sup>1</sup>

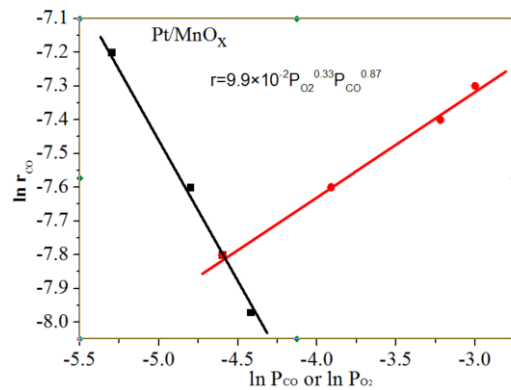


Figure. S7 Reaction kinetics of CO oxidation. Reaction rates ( $r_{CO}$ ) as a function of CO or O<sub>2</sub> concentration over Pt/MnO<sub>x</sub> catalyst: (black line) CO and (red line) O<sub>2</sub>.

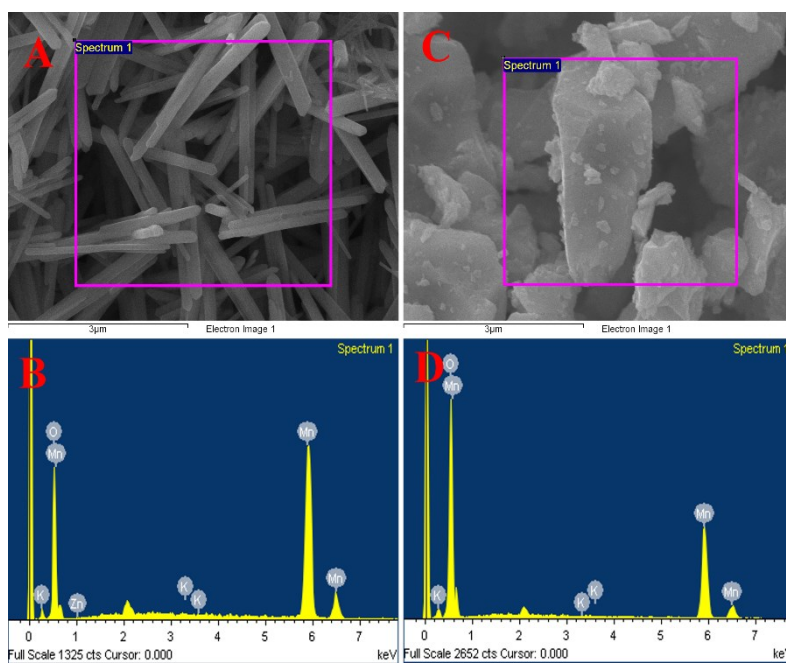


Figure S8. SEM and EDX of  $\beta$ -MnO<sub>2</sub> (A, B) and  $\beta$ -MnO<sub>2</sub>-COM (C, D).

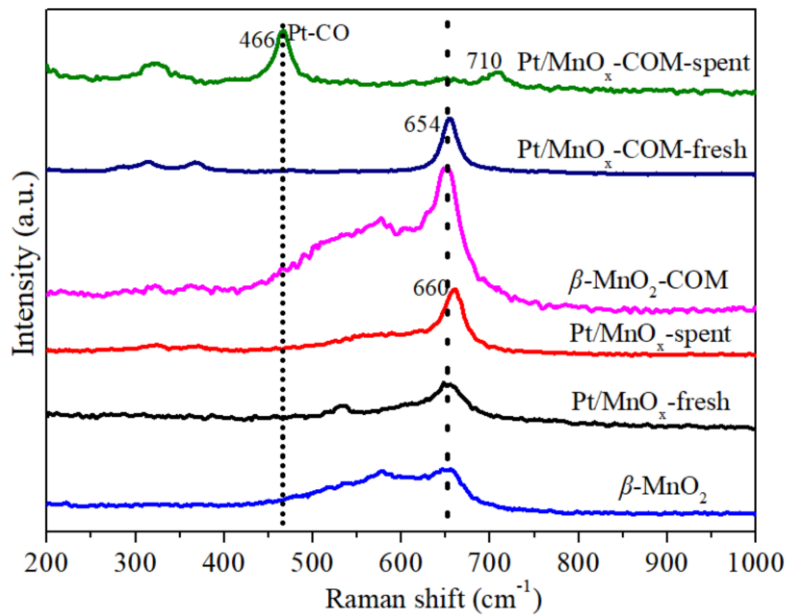


Figure S9. Raman spectra of the catalysts.

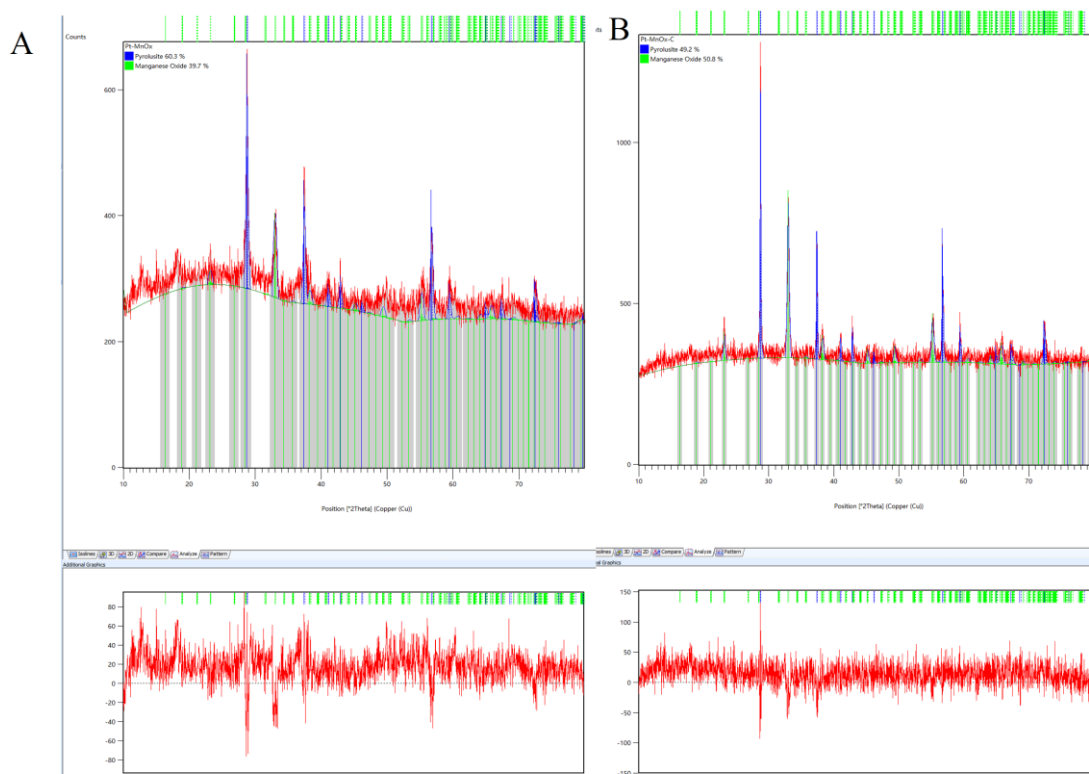


Figure S10. Rietveld refinement for the spent catalysts: (A) Pt/MnO<sub>x</sub>; (B) Pt/MnO<sub>x</sub>-COM

### 3. Tables

Table S1.  $T_{10}$ ,  $T_{50}$ , and  $T_{90}$  of CO oxidation over the catalysts.

Sample	$T_{10}$ (°C)	$T_{50}$ (°C)	$T_{90}$ (°C)
$\beta$ -MnO <sub>2</sub>	120	180	> 200
Pt/MnO <sub>x</sub>	73 (rough)	82 (rough)	96 (rough)
$\beta$ -MnO <sub>2</sub> -COM	168	> 200	> 200
Pt/MnO <sub>x</sub> -COM	140	160	175 (rough)

Table S2. Reaction rate ( $r$ ), turnover frequency (TOF), apparent activation energy ( $E_a$ ) and pre-exponential factor for CO oxidation over Pt/MnO<sub>x</sub> and Pt/MnO<sub>x</sub>-COM catalysts.

Temperature (°C)	<sup>a</sup> Reaction rate (mol <sub>co</sub> g <sup>-1</sup> s <sup>-1</sup> )		<sup>b</sup> TOF s <sup>-1</sup>			
	Pt/MnO <sub>x</sub>	Pt/MnO <sub>x</sub> -COM	Pt/MnO <sub>x</sub>	Pt/MnO <sub>x</sub> -COM	Pt/ 3 DOM MnO <sub>x</sub>	Pt/Al <sub>2</sub> O <sub>3</sub>
100	1.67×10 <sup>-6</sup>	0	9.1×10 <sup>-2</sup>			
120		2.77×10 <sup>-7</sup>		2.5×10 <sup>-2</sup>		
150	5.03×10 <sup>-6</sup>	6.16×10 <sup>-7</sup>	2.74×10 <sup>-1</sup>	5.6×10 <sup>-2</sup>	2.72×10 <sup>-1</sup>	3.01×10 <sup>-2</sup>
200	7.50×10 <sup>-6</sup>	1.8×10 <sup>-7</sup>	4.09×10 <sup>-1</sup>	1.71×10 <sup>-1</sup>		
250	1.17×10 <sup>-6</sup>	5.03×10 <sup>-7</sup>	6.38×10 <sup>-1</sup>	4.62×10 <sup>-1</sup>		
$E_a$ (kJ mol <sup>-1</sup> )	20.5	1.39×10 <sup>-3</sup>				
A (mol g <sup>-1</sup> s <sup>-1</sup> )	38.37	3.32×10 <sup>-2</sup>				

<sup>a</sup> The reaction rates were measured with a feed stream of 0.5% CO/0.5O<sub>2</sub>/He, and the space velocity in the range of 1.5×10<sup>5</sup>-2.1×10<sup>6</sup> ml g<sup>-1</sup> h<sup>-1</sup>, through which the conversion of CO was adjusted to below 15% in order to calculate the reaction rates under differential reactor conditions.

<sup>b</sup> The degree of metal dispersion calculated from CO chemisorption 43.5% and 25.1% for the Pt/MnO<sub>x</sub> and Pt/MnO<sub>x</sub>-COM, respectively.

Table S3. Surface information of the fresh and used catalysts

Sample	adsorbed oxygen (%)		lattice oxygen (%)	Mn <sup>3+</sup> (%)	Mn <sup>4+</sup> (%)	Pt <sup>2+</sup> (%)	Pt <sup>4+</sup> (%)
	hydrated/carbonated oxygen species	adsorbed surface oxygen species					
	$\beta$ -MnO <sub>2</sub> -fresh	0					
$\beta$ -MnO <sub>2</sub> -spent	0	51.2	48.8	42.8	57.2	0	0
Pt/MnO <sub>x</sub> -fresh	7.8	46.3	45.9	36.1	63.9	66.4	33.6
Pt/MnO <sub>x</sub> -spent	14.6	35.9	49.5	67.1	32.9	62.9	37.1
Pt/MnO <sub>x</sub> -COM-fresh	4.6	47	48.4	30.2	69.8	67.5	32.5
Pt/MnO <sub>x</sub> -COM-spent	6.66	38.7	54.7	56.1	43.9	63.9	36.1

Table S4. EXAFS fitting parameters at the Pt LIII-edge for Pt-based catalysts

Sample	Shell	CN <sup>a</sup>	R (Å) <sup>b</sup>	$\sigma^2$ (Å <sup>2</sup> ·10 <sup>3</sup> ) <sup>c</sup>	$\Delta E_0$ (eV) <sup>d</sup>	R factor (%)
Pt/MnO <sub>x</sub>	Pt–O	6.1	2.00	3.5	11.9	0.3
Pt/MnO <sub>x</sub> -C	Pt–O	5.7	2.00	2.8	10.3	0.4
Pt foil	Pt–Pt	12.0	2.77	4.9	8.7	0.11
PtO <sub>2</sub>	Pt–O	6.0	2.02	2.9	11.2	0.4

<sup>a</sup> CN: coordination numbers; <sup>b</sup> R: bond distance; <sup>c</sup>  $\sigma^2$ : Debye–Waller factors; <sup>d</sup>  $\Delta E_0$ : the inner potential correction. S02 for Pt–Pt is 0.87, for Pt–O is 0.84, were obtained from the experimental EXAFS fit of Pt foil / PtO<sub>2</sub> references by fixing CN as the known crystallographic value and were fixed to the two catalysts.

Table S5. Rietveld refined XRD parameters of fresh and spent Pt-based catalysts

sample	Pt/MnO <sub>x</sub> -fresh	Pt/MnO <sub>x</sub> -spent	Pt/MnO <sub>x</sub> -COM-fresh	Pt/MnO <sub>x</sub> -COM-spent	
<b>Phase contents</b>					
MnO <sub>2</sub>	23.2%	60.3%	21.8%	49.2%	
Mn <sub>2</sub> O <sub>3</sub>	76.8%	39.7%	78.2%	50.8%	
<b>Space group</b>					
MnO <sub>2</sub>	P42/mnm (136)	P42/mnm (136)	P42/mnm (136)	P42/mnm (136)	
Mn <sub>2</sub> O <sub>3</sub>	Pbca (61)	Pbca (61)	Pbca (61)	Pbca (61)	
<b>Cell parameters</b>					
MnO <sub>2</sub>	a (Å)	4.3980	4.4000	4.3977	4.3985
	c (Å)	2.8724	2.8720	2.8725	2.8731
Mn <sub>2</sub> O <sub>3</sub>	a (Å)	4.4104	9.3958	9.4089	9.3857
	b (Å)	4.4105	9.3989	9.4114	9.4081
	c (Å)	9.4144	9.4455	9.4129	9.4491
<b>R-factors</b>					
R <sub>exp</sub> (%)	4.2	6.0	4.2	5.3	

R <sub>p</sub> (%)	4.4	6.5	5.1	4.9
R <sub>wp</sub> (%)	5.9	7.6	7.0	5.9
GOF-index	1.9	1.6	2.8	1.3

---

Table S6. Chemical Compositions of Supports (EDX)

Support Elements	$\beta$ -MnO <sub>2</sub> (weight %)	$\beta$ -MnO <sub>2</sub> (Atomic%)	$\beta$ -MnO <sub>2</sub> -COM (weight %)	$\beta$ -MnO <sub>2</sub> -COM (Atomic%)
Mn	84	60	68	38
O	16	40	32	62
K	0	0	0	0
Zn	0	0.01	0	0

---